MPMI Vol. 9, No. 7, 1996, pp. 546–555. Publication no. M-1996-0708-01R.

Nodule Development Induced by Mutants of *Bradyrhizobium japonicum* Defective in Cyclic *B*-glucan Synthesis

John Dunlap[1], Eiichi Minami[2,3], Arvind A. Bhagwat[4,5], Donald L. Keister[4], and Gary Stacey[2]

[1]Department of Botany, 437 Hesler Biology Building, The University of Tennessee, Knoxville 37996 U.S.A.; [2]Center for Legume Research, Departments of Microbiology and Ecology and Evolutionary Biology, M409 Walters Life Science Building, The University of Tennessee, Knoxville 37996-0845 U.S.A.; [3]Department of Cell Biology, National Institute of Agrobiological Resources, Tsukuba, Ibaraki, 305, Japan; [4]Soybean and Alfalfa Research Laboratory, USDA-ARS, Bldg. 011, HH-19, BARC-W, Beltsville, MD 20705 U.S.A.; [5]Department of Agronomy, University of Maryland, College Park 20742 U.S.A.

Received 3 April 1996. Accepted 4 June 1996.

The soybean response to inoculation with *B. japonicum* mutants defective in cyclic β-(1→3), β-(1→6) glucan synthesis was examined by electron microscopy and by monitoring the expression of early and late nodulin genes. Two mutants were examined. Strain AB-14 is an *ndvB* mutant and is unable to synthesize β-glucans. Strain AB-1 is an *ndvC* mutant and produces cyclic glucans containing 95 to 100% β-(1→3) glycosidic linkages. Nodules formed by either mutant were defective in nitrogen fixation activity. Soybean plants inoculated with strain AB-14 formed nodules roughly at the same rate as the wild-type strain USDA110, but nodulation by strain AB-1 was significantly delayed. Microscopy of nodules formed by strain AB-14 showed an overall ultrastructure similar to nodules formed by the wild type. However, in some nodules bacteroids were limited to only one part of the infected cells and in others the few bacteroids present showed signs of degradation. Nodulelike structures were formed by strain AB-1 that showed some signs of cellular differentiation. For example, clear parenchyma and sclerenchyma tissue could be seen. However, no infection threads or bacteria were evident in these structures. The expression of early (e.g., ENOD2 and ENOD55) and late (e.g., NOD26 and leghemoglobin) nodulins was examined. Nodules formed by strain AB-14 expressed all of the nodulins tested but at a reduced level. Expression of late nodulins was delayed in strain AB-14–induced nodules. Nodules formed by strain AB-1 were more strongly affected in nodulin expression. Although leghemoglobin synthesis was not detected, infection-specific nodulin transcripts of *Gm*N93 and ENOD55 were detected. However, expression of the early nodulins ENOD2 and ENOD55 was considerably delayed and only apparent when assayed 21 days postinoculation. A low level of expression of intermediate nodulin *Gm*N70 and late nodulin NOD26 could also be detected by 21 days postinoculation. The microscopy data show that tissue differentiation occurs in these nodules even in the absence of active bacterial invasion. These results demonstrate the importance of cyclic β-(1→3), β-(1→6) glucan synthesis to symbiotic development in soybean.

Corresponding author: Gary Stacey, Center for Legume Research, M409 Walters Life Science Building, The University of Tennessee, Knoxville 37996-0845; Tel. 615-974-4041; FAX 615-974-4007; E-mail: GSTACEY@utk.edu

Microorganisms belonging to the family *Rhizobiaceae* are well known for their symbiotic and pathogenic interactions with host plants. Cell-associated carbohydrates of these bacteria have been shown to provide important function(s) during the plant infection process. Cyclic β-glucans are synthesized by all species of *Rhizobium, Bradyrhizobium,* and *Agrobacterium* examined (Breedveld and Miller 1994). Cyclic β-glucans play an important role in hypoosmotic adaptation and have been suggested to have a more specific role in legume infection (Dylan et al. 1990a; Breedveld and Miller 1994).

Cyclic β-glucans of *Rhizobium* and *Agrobacterium* species principally are composed of 17 to 25 glucose residues linked by β-(1→2)-D-glycosidic bonds and may be substituted with phosphoglycerol and/or succinate (York et al. 1978; Bately et al. 1987; Hisamatsu et al. 1987). Two genes from *Rhizobium meliloti* have been identified for synthesis and transport of cyclic β-(1→2)-glucans. The *ndv*B gene encodes a glucan synthetase that is 319 kDa (Ielpi et al. 1990). The second gene, *ndv*A, is postulated to encode a transporter that allows cyclic β-glucans to move from the cytoplasm to the periplasmic space (Stanfield et al. 1988). *R. meliloti* mutants defective in NdvA or NdvB function exhibit a pleiotropic phenotype (Dylan et al. 1990a; Ielpi et al. 1990). Among the phenotypic changes are loss of motility, increased resistance to bacteriophage lysis, and increased sensitivity to certain antibiotics. The *ndvB* mutants induced the formation of nodulelike structures on alfalfa roots that were lacking infecting bacteria or a visible infection thread (Dylan et al. 1986). Regarding this phenotype, *ndvB* mutants resemble *R. meliloti* mutants unable to produce an acidic exopolysaccharide (Finan et al. 1985; Leigh et al. 1985) or that produce an altered exopolysaccharide (Leigh et al. 1987). Symbiotic pseudorevertants of the *R. meliloti ndvB* mutants have been isolated (Dylan et al. 1990b).

These pseudorevertants were still unable to synthesize a periplasmic β-(1→2)-cyclic glucan but regained some symbiotic ability. Curiously, these pseudorevertants formed normal nodules on approximately one in 10 alfalfa plants inoculated, but continued to form uninfected nodulelike structures on the remaining plants. These data would suggest that cyclic β-(1→2)-glucan is not essential for nodulation, but clearly plays an important role. However, it was also observed that inclusion of physiological levels (6 and 32 μM) of cyclic β-(1→2)-glucans during inoculation of seedlings with wild-type *R. meliloti* enhanced nodulation kinetics and doubled nodule number, suggesting that β-glucans may function as signal molecules and/or are involved in optimizing nodulation (Dylan et al. 1990b).

B. japonicum does not synthesize cyclic β-(1→2)-glucans. Instead, cyclic β-(1→3), β (1→6)-glucans, composed of 11 to 13 glucosyl residues, are produced that may also be substituted with phosphocholine (Rolin et al. 1992). Although the *Rhizobium* and *Bradyrhizobium* periplasmic glucans are structurally different, they appear to be functional analogs, at least in osmoregulation (Miller and Gore 1992; Bhagwat et al. 1993). Using this observation, Bhagwat et al. (1993) were able to isolate a *B. japonicum* DNA locus for β-(1→3), β (1→6)-glucan synthesis by functional complementation of a *R. meliloti ndvB* mutant for hypoosmotic growth and symbiotic interaction with alfalfa. Subsequent mutagenesis of the *B. japonicum ndvB* locus resulted in mutants unable to produce cyclic glucans and with a pleiotropic phenotype, including loss of motility, poor growth under low osmolarity, and formation of ineffective (i.e., unable to fix nitrogen) nodules on soybean (Bhagwat and Keister 1995). Using site-directed Tn*5* mutagenesis, the *ndvC* gene, adjacent to the *ndvB* gene (Bhagwat et al., in press), was identified and a mutant was obtained (i.e., strain AB-1; Bhagwat et al., in press). The *ndvC* gene is predicted to encode a 62-kDa membrane protein. Unlike the wild type, a mutant defective in NdvC produces cyclic glucans containing 95 to 100% β(1-3) glycosidic linkages. In addition, the mutant shows a slight sensitivity to hypoosmotic growth conditions, is motile, but is severely impaired in the ability to nodulate soybean plants.

Rhizobium and *Bradyrhizobium* mutants defective in normal nodule formation can be used as tools to examine nodule development. For example, *R. meliloti* mutants defective in exopolysaccharide synthesis have been shown to form empty nodules, similar to *ndvB* mutants, but still induce the early nodulin, ENOD2 (van de Wiel et al. 1990a). These results clearly show that infection is not required for the induction of this early nodulin. As shown below, we have examined nodules induced by *B. japonicum ndvB* and *ndvC* mutants and have used these mutants as tools to examine nodulin gene expression. The results show that tissue differentiation does occur and nodulelike structures are formed even in the absence of bacterial infection. This conclusion is supported by ultrastructural analysis, and by the expression of late nodulins previously thought to require bacterial invasion for expression.

RESULTS

Microscopy of nodules induced by mutant strains AB-1 and AB-14.

Considering the possibility that β-glucans may act as signal compounds during the plant infection process, we analyzed the host response to inoculation with *B. japonicum* glucan mutants AB-1 and AB-14 by electron microscopy and by monitoring the expression of early and late nodulin genes.

G. max cv. Essex plants inoculated with wild-type strain USDA110 or the NdvB$^-$ mutant, strain AB-14, formed nodules at approximately the same rate. Visible structures were apparent 8 days postinoculation (PI). In contrast, soybean plants inoculated with mutant strain AB-1 (NdvC$^-$) did not form visible nodules until 14 days PI. In contrast to the wild type, the mutant nodules formed primarily on lateral roots. Acetylene reduction assays failed to detect nitrogen fixation activity in nodules formed by either the *ndvB* or *ndvC* mutant over the course of the experiment (i.e., until 21 days PI, data not shown).

Nodules formed by the wild type.

At 14 days PI, the wild-type strain USDA110 induced roughly spherical nodules with a diameter of 1 to 2 mm (Fig. 1A) and had a large, prominent, central region of infected and uninfected cells. The infected cells were large with an evenly dispersed cytoplasm, whereas the uninfected cells were small with a large, central vacuole (Fig. 1B). The central region of tissue was surrounded by layers of parenchyma and sclerenchyma. The nodule inner and outer cortex layers were of variable thickness and were separated by a single cell layer of sclerenchyma.

The infected cells were typically 15 to 20 μm in diameter with bacteroids evenly dispersed within the cell. The nucleus was medially located; mitochondria and plastids were found along the margin of the cell (Fig. 1C), and Golgi and endoplasmic reticulum (ER) profiles were randomly dispersed throughout the cytoplasm. Although plastids were sometimes present, starch grains were rare in these cells. Most infected cells had cytoplasmic vesicles containing loosely organized fibrillar material. Uninfected cells typically contained one large, central vacuole that compressed the cytoplasm into a thin layer along the margin of the cell. Starch grains, if present, accumulated in the uninfected cells.

By 21 days PI, nodules induced by the wild type were typically 2 to 3 mm in diameter and the general tissue organization appeared like that observed at 14 days PI. However, the number of bacteria within a cell and the number of infected cells within the nodule had markedly increased. The average infected cell diameter increased to approximately 30 μm (Fig. 1D) and cytoplasmic vesicles were no longer obvious. As is typical of *B. japonicum*–induced nodules, each symbiosome typically contained several bacteroids that were beginning to accumulate polyhydroxybutyrate granules by 21 days PI (Fig. 1E). Fine granular material was also common within the symbiosome by 21 days PI (Fig. 1E).

Nodules induced by mutant strain AB-14 (*ndvB*).

In nodules induced by strain AB-14 (*ndvB*), the general tissue organization was similar to that found in wild type–induced nodules. Layers of parenchyma, separated by a layer of sclerenchyma, surrounded the prominent central region (Fig. 2A). Some cells in the central region were larger, with evenly dispersed cytoplasm, and lacked a large, central vacuole, all features characteristic of infected cells in wild type–induced nodules. There were also smaller cells that possessed a single, large, central vacuole typical of uninfected cells.

At 14 days PI, two ultrastructurally distinct types of nodules were apparent. In one, few if any bacteria were present in what appeared to be infected cells (Fig. 2B–D). In this case, we define the infected cell as lacking a large, central vacuole, having a densely stained, uniformly dispersed cytoplasm, and being larger in diameter than the typical uninfected cell. These infected cells tended to be rounded and had an average diameter of approximately 25 μm (Fig. 2C). Their cytoplasm was vesiculate; however, the number and size of vesicles both within and from cell to cell was quite diverse (Fig. 2C). The vesicles contained loosely organized fibrillar material (Fig. 2D). Plastids and starch grains were evident along the periphery of both infected and uninfected cells and peroxisomes were evident in the uninfected cells (data not shown). Closer examination of the bacteria released from an infection thread showed them to be typically in some stage of degradation (Fig. 2D). These bacteria were generally not surrounded by a symbiosome membrane.

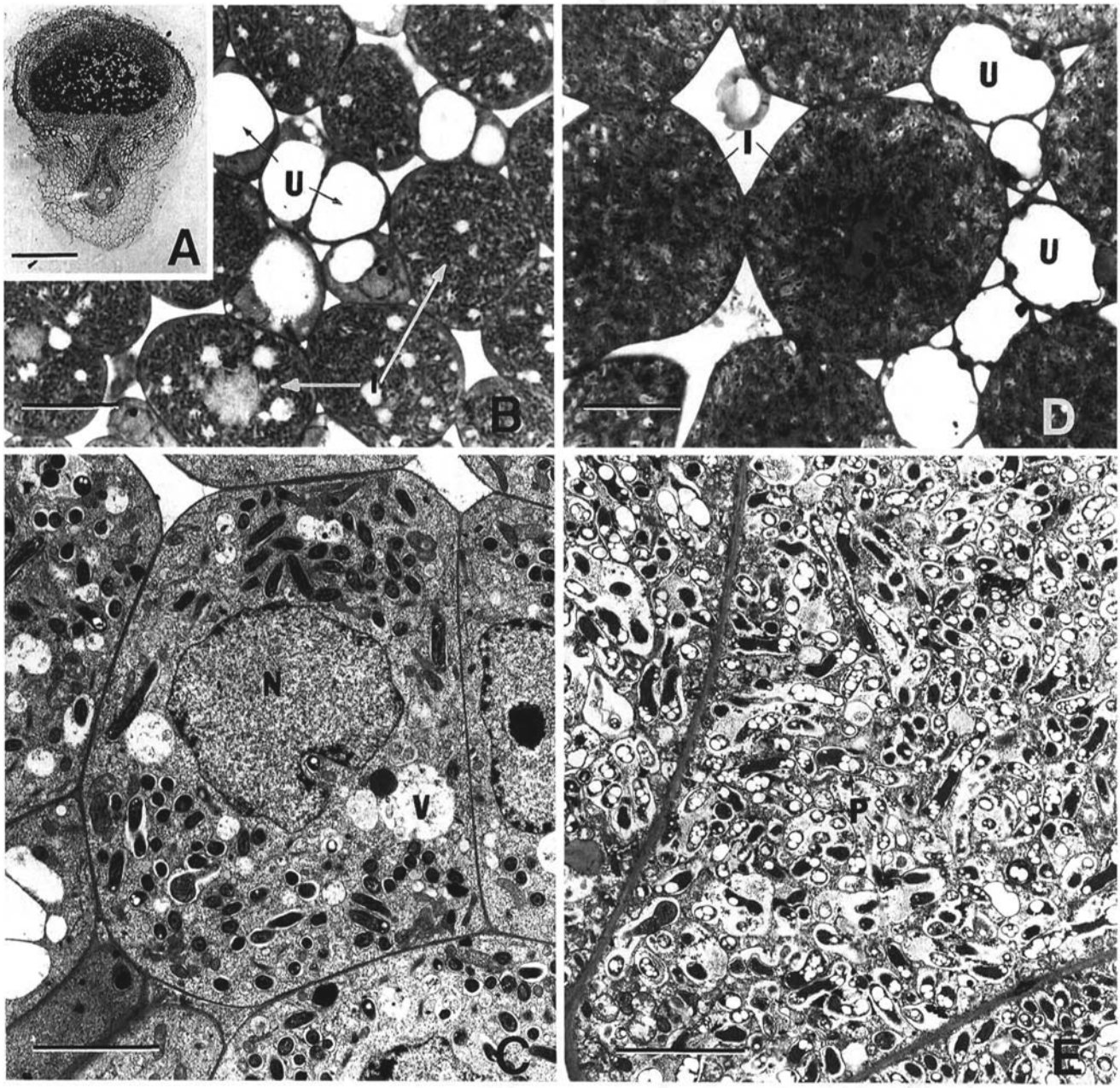

Fig. 1. Light (LM) and transmission electron micrographs (EM) of soybean nodules at 14 days (**A, B,** and **C**) and 21 days (**D** and **E**) postinoculation (PI) with *Bradyrhizobium japonicum* wild-type strain USDA110. Abbreviations: B, bacteroid; CW, cell wall; IT, infection thread; I, infected cell; N, nucleus; P, polyhydroxybutyrate; S, starch; U, uninfected cell; V, vesicle. **A,** LM of 14 days PI nodule showing the size, shape, and tissue differentiation characteristic of a wild-type infection. Bar = 0.5 mm. **B,** LM showing general arrangement of infected and uninfected cells. Bar = 20 μm. **C,** EM of an infected cell showing even distribution of bacteroids, central location of nucleus, and lack of a large, central vacuole. Bar = 5 μm. **D,** LM of 21 days PI nodule showing general features of uninfected and infected cells; the latter is greatly enlarged from 14 days PI. Bar = 20 μm. **E,** EM of infected cell revealing multiple bacteroids per symbiosome and accumulation of polyhydroxybutyrate in bacteroids. Bar = 5 μm.

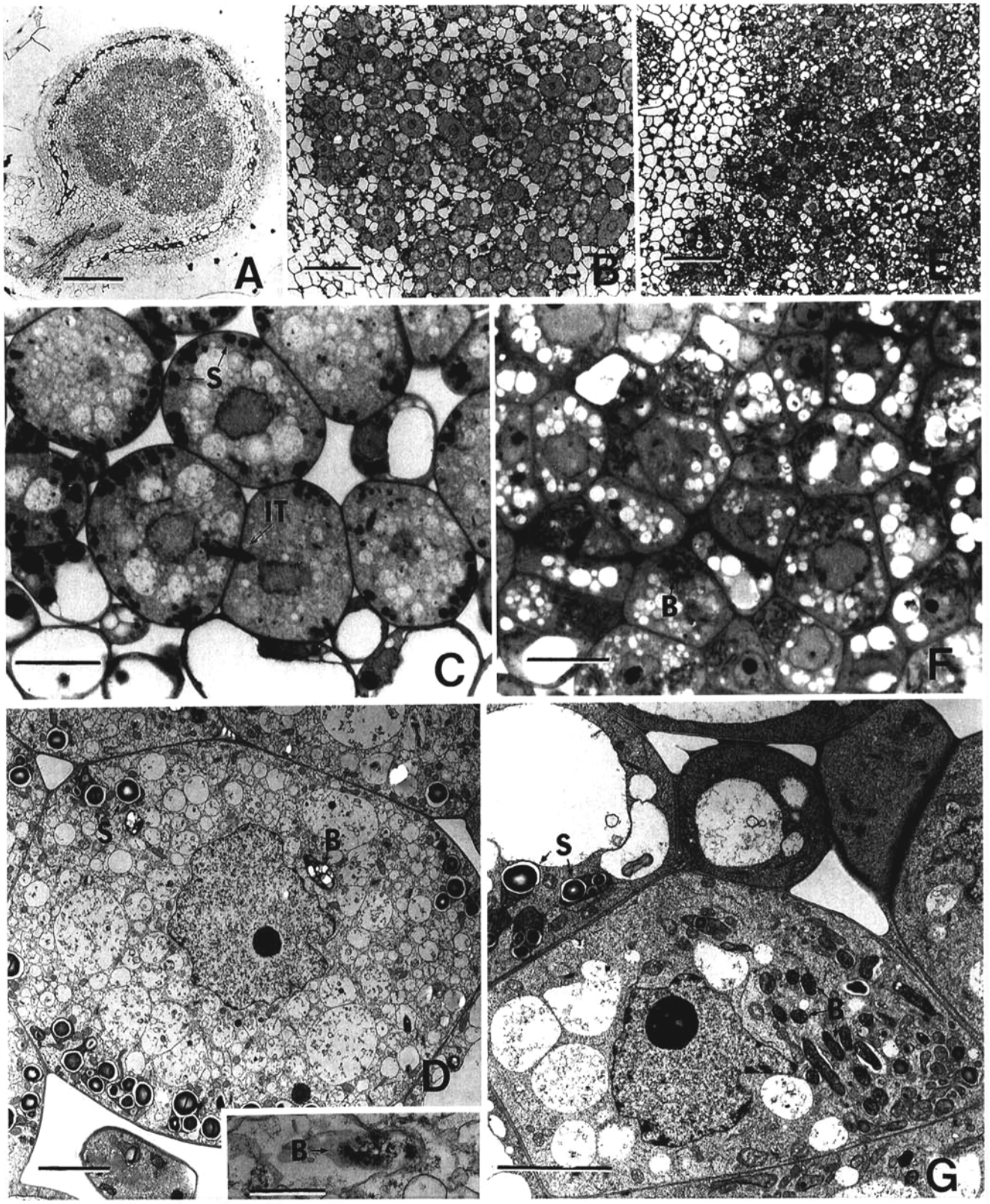

Fig. 2. Light (LM) and transmission electron (EM) micrographs of soybean nodules at 14 days postinoculation (PI) with the *ndvB* mutant strain AB-14. Abbreviations as in Figure 1. **A,** LM showing that nodule morphology is generally like that of wild type–induced nodules. Bar = 0.5 mm. **B,** LM showing general arrangement of infected and uninfected cells in central region of the nodule. Bar = 95 μm. **C,** LM showing even distribution of cytoplasms in infected cells and accumulation of starch in infected and uninfected cells. Bar = 20 μm. **D,** EM of an infected cell showing rounded nature of cell, accumulation of starch along edge of cell, and almost complete lack of bacteroids. Bar = 5 μm. **D,** Inset: EM of a bacteroid from a cell like that shown in **D,** showing state of degradation of bacteroid. Bar = 1 μm. **E,** LM of a second class of nodules resulting from infection by strain AB-14 showing the general arrangement of cells in central region of nodule. Bar = 95 μm. **F,** LM showing degree of vesiculation in both infected and uninfected cells and presence of bacteroids. Bar = 20 μm. **G,** EM showing presence and clustering of bacteroids in infected cell and presence of starch in uninfected cell. Bar = 5 μm.

In a second and less frequent type of nodule induced by strain AB-14, bacteria were present in the infected cells. At low magnification, the central region of the nodule had a lacy appearance due to the high degree of vesiculation in both infected and uninfected cells (Fig. 2E, F). At 20 μm in diameter, the infected cells were slightly smaller than infected cells of the same age from the other nodule type induced by the *ndvB* mutant (compare Fig. 2C and F). When bacteria were present, they were localized to one area of the cell (Fig. 2F and G). Although plastids were present, very few starch grains were found in infected cells. Some cells within the central region appeared to share characteristics of both infected and uninfected cell types. These cells were smaller than infected cells, had multiple, large, empty vacuoles and lacked bacteria (Fig. 2F and G). Starch grains, if present, were found in this latter cell type.

Although there were two types of nodules on plants inoculated by strain AB-14 at 14 days PI, this was not the case by 21 days PI. The nodules present at 21 days PI shared characteristics of both types observed at 14 days PI. The overall nodule size increased by 21 days PI and the infected cell size was approximately 35 μm. There were more infected cells and

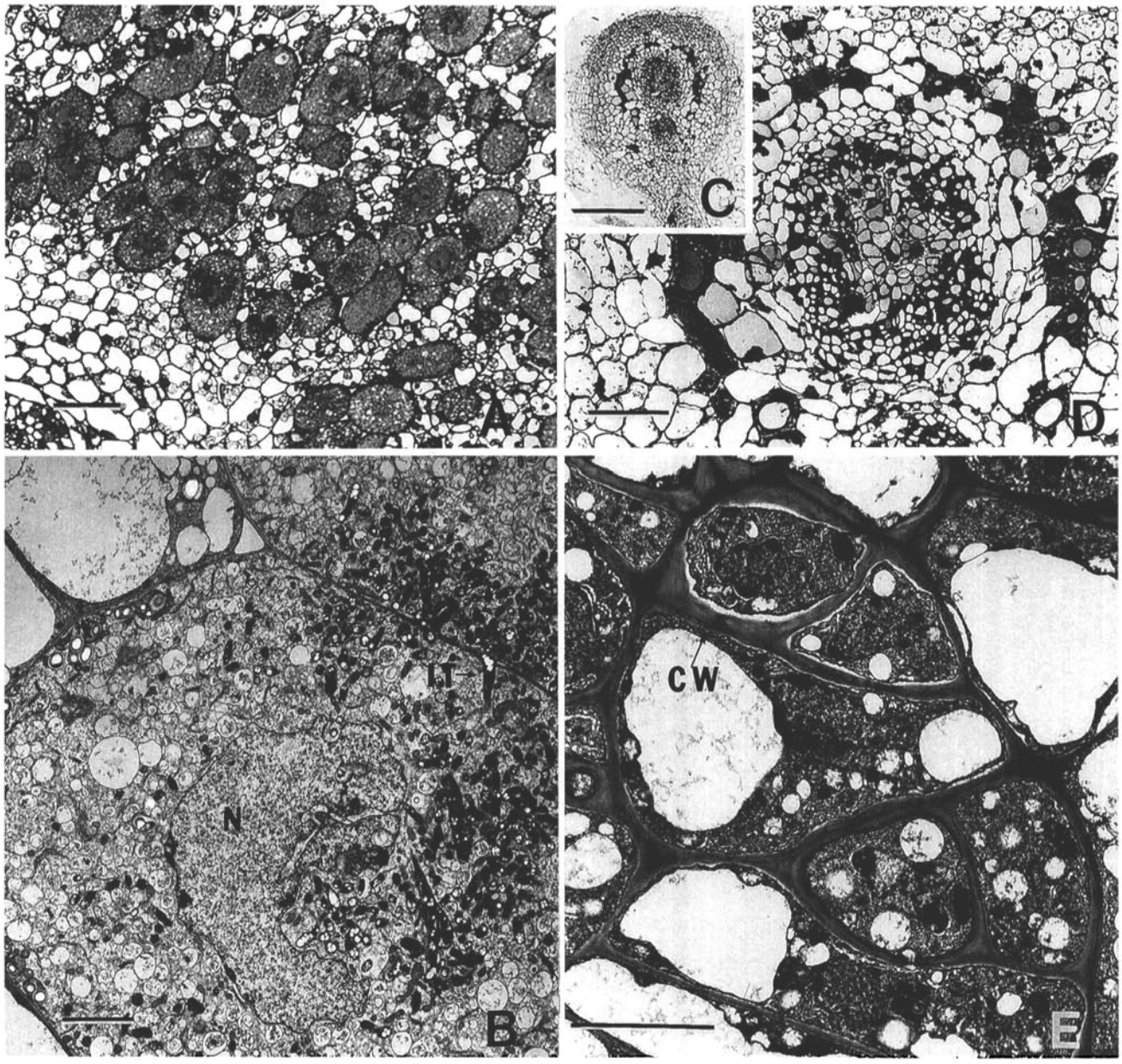

Fig. 3. Light (LM) and transmission electron (EM) micrographs of soybean nodules at 21 days postinoculation (PI) with either *ndvB* mutant strain AB-14 (**A** and **B**) or *ndvC* mutant strain AB-1 (**C, D,** and **E**). Abbreviations as in Figure 1. **A,** LM from central region of a nodule showing distribution of infected and uninfected cells and rounded nature of infected cells. Bar = 50 μm. **B,** EM showing clustered distribution of bacteroids in infected cell and continued accumulation of starch along margin of cell. Bar = 5 μm. **C,** LM showing morphology of nodulelike structure induced by *ndvC* mutant strain AB-1. Bar = 0.5 mm. **D,** LM through central region of nodulelike structure showing some cellular differentiation. Bar = 50 μm. **E,** EM from central region showing increase in cell wall thickness and cytoplasm density and vacuole size characteristic of infected and uninfected cells. Bar= 5 μm.

the number of bacteria within these cells had increased. The bacteria, however, still were localized to a small area of the cell and, when a neighboring cell was infected, the sites of infection for the two cells were adjacent (Fig. 3A and B). Infected cells remained highly vesiculate, cytoplasmic organelles were easily visualized, and starch grains continued to accumulate along the periphery of both infected and uninfected cells (Fig. 3B). Peroxisomes were still evident in the uninfected cells.

Nodules induced by mutant strain AB-1 (*ndvC*).

Nodulation by strain AB-1 (*ndvC*) was rare at 14 days PI; however, by 21 days PI some nodulelike structures were present. These small, white nodules typically formed at the base of a lateral root. Sections through these nodules (Fig. 3C) showed them to be roughly spherical and approximately 0.9 mm in diameter, with a tissue organization resembling wild type–induced nodules. For example, there were layers of parenchyma separated by a layer of sclerenchyma. There was also some degree of cellular differentiation in the central region of the nodule (Fig. 3D, E). Cells within this region could be differentiated into two types: (i) those with a large, central vacuole that forced the cytoplasm into a narrow band along the margin of the cell (features of uninfected cells) and (ii) those without a large, central vacuole and with densely stained, evenly dispersed cytoplasm (features of infected cells). Thickened cell walls were common in both cell types (Fig. 3E). Neither infection threads nor bacteria were evident in these structures.

Nodulin gene expression in nodules induced by *B. japonicum* AB-1 and AB-14 mutants.

Although microscopy is useful for defining the morphological development of nodules, this technique does not allow a molecular analysis of development. In order to characterize further nodules formed by either the *ndvB* or *ndvC* mutant, we sought to use nodulin gene expression as a tool to characterize the degree of nodule development. We used a variety of nodulins induced at different times during normal nodule ontogeny. Figure 4 summarizes this work. We used reverse transcription–polymerase chain reaction (RT-PCR) to characterize these nodules, since this method has a high degree of sensitivity and was particularly valuable in the case of AB-1–induced nodules, where little nodule tissue was available. This method can be used for quantitative measurements of the relative levels of gene transcripts by the inclusion of a constitutively expressed internal control. In our case, ubiquitin mRNA was simultaneously amplified as the internal control. In each case, the signal intensities from hybridization to the nodulin probes can be standardized by comparison with the control ubiquitin hybridizations shown (Fig. 4).

Total RNA was collected at various times PI and amplified by RT-PCR. As can be seen in Figure 4, in every case, nodulin expression was detected in nodules induced by the wild type, strain AB-14 (*ndvB*), and strain AB-1 (*ndvC*). However, in the case of nodules formed by the *ndvB* or *ndvC* mutants, there was an apparent delay in nodulin gene expression. These results are consistent with the microscopic analysis that indicated a delay in nodule development. In the case of the early nodulins, ENOD2 and ENOD55-1, mRNA accumulation could be detected in nodules induced by both the wild type and strain AB-14 (*ndvB*) by 8 days PI, the earliest time point tested (Fig, 4A, C). However, the expression in the AB-14–induced nodules appeared to be reduced, relative to those induced by the wild type. This was also the case for nodulin *Gm*N93 (Fig. 4E), which can be classified as an early nodulin, normally expressed within 3 days PI (Kouchi and Hata 1993). A clearer delay can be seen in the expression of the intermediate nodulin *Gm*N70, first appearing in wild-type nodules at 5 to 6 days PI (Kouchi and Hata 1993), and the late nodulin NOD26, in which, in contrast to the wild type, no expression in nodules induced by strain AB-14 (*ndvB*) was observed until sampled at 14 days PI (Fig. 4B, D).

Consistent with the microscopic analysis, the nodulelike structures formed by mutant stain AB-1 (*ndvC*) were more strongly affected in nodulin expression. Expression of the early nodulins, ENOD2 and ENOD55-1, was not detected at 14 days but was apparent when sampled at 21 days PI (Fig. 4A, C). Considering this extensive delay in early nodulin expression, it was surprising to find the expression of intermediate nodulin *Gm*N70 by 21 days PI (Fig. 4D). Indeed, the late nodulin, NOD26, is also expressed in nodules induced by strain AB-1 by 21 days PI (Fig. 4B). Thus, although the nodulelike structures formed by the AB-1 mutant are grossly affected morphologically, they appear to express all of the nodulins tested, but with a considerable delay. The one exception is Lba, which was absent from nodules induced by strain AB-1 (Fig. 4F).

DISCUSSION

Analysis of nodulin gene expression enabled us to differentiate host interaction with two *ndv* mutants of *B. japonicum*. Strain AB-14 (*ndv*B) is unable to synthesize any glucans under in vitro or in vivo conditions. Strain AB-1 carries a Tn*5* insertion mutation in the *ndvC* gene and as a result produces a novel β-glucan species having 95 to 100% β-(1→3) linkages. Although both strains formed symbiotically ineffective (Fix^-) nodules on soybean, their interactions are arrested at different stages of nodule morphogenesis.

The nodules induced by these mutants showed a range of morphological responses. Nodules induced by the *ndv*B mutant strain AB-14 showed normal tissue differentiation by 14 days PI. Infection threads were apparent, as were bacteroids. However, in this case normal tissue differentiation does not correlate with normal (i.e., Fix^+) nodule function. Nodules formed by mutant AB-14 appeared morphologically and physiologically normal but, even when infected bacteria were present, they were defective in nitrogen fixation ability. Ultrastructurally, at 14 days PI the nodules had abnormalities that correlated with the lack of nitrogen fixation. For example, ineffective nodules can be characterized by the presence of starch grains, the high degree of infected cell vesiculation, and the degradation of bacteria once released from the infection thread (e.g., Rossbach et al. 1989; Roth and Stacey 1992). Fortin et al. (1987) reported similar results and attributed the apparent degradation of bacteroids to the lack of a symbiosome membrane. In this case, mutant bacteria were released from the infection thread into a differentiated cell but quickly degraded. However, Fortin et al. (1987) found significant levels of nodulin 26 expression in these mutant nodules. The results from our work corroborate these findings in that nodules

induced by strain AB-14 were unable to fix nitrogen (as measured by acetylene reduction at 14 and 21 days PI), but did express nodulin 26 and had differentiated tissue. As further support of cellular differentiation in the AB-14–induced nodules, we found that Lba, which is considered a marker for the differentiated infected cell type within the nodule, was expressed at normal levels.

R. meliloti ndv mutants are severely retarded in their ability to attach and induce infection thread formation (Dylan et al. 1990b). However, the primary block to symbiosis in these mutants is thought to occur subsequent to attachment and infection thread development. Even in *R. meliloti*–symbiotic pseudorevertant strains of *ndv* mutants (Dylan et al. 1990b), attachment and infection thread development was little better than in the original mutants. By 21 days PI, however, nodulation rates with the *ndvB* symbiotic pseudorevertants were similar to those induced by the wild-type bacteria. These data are consistent with those from the present study in that

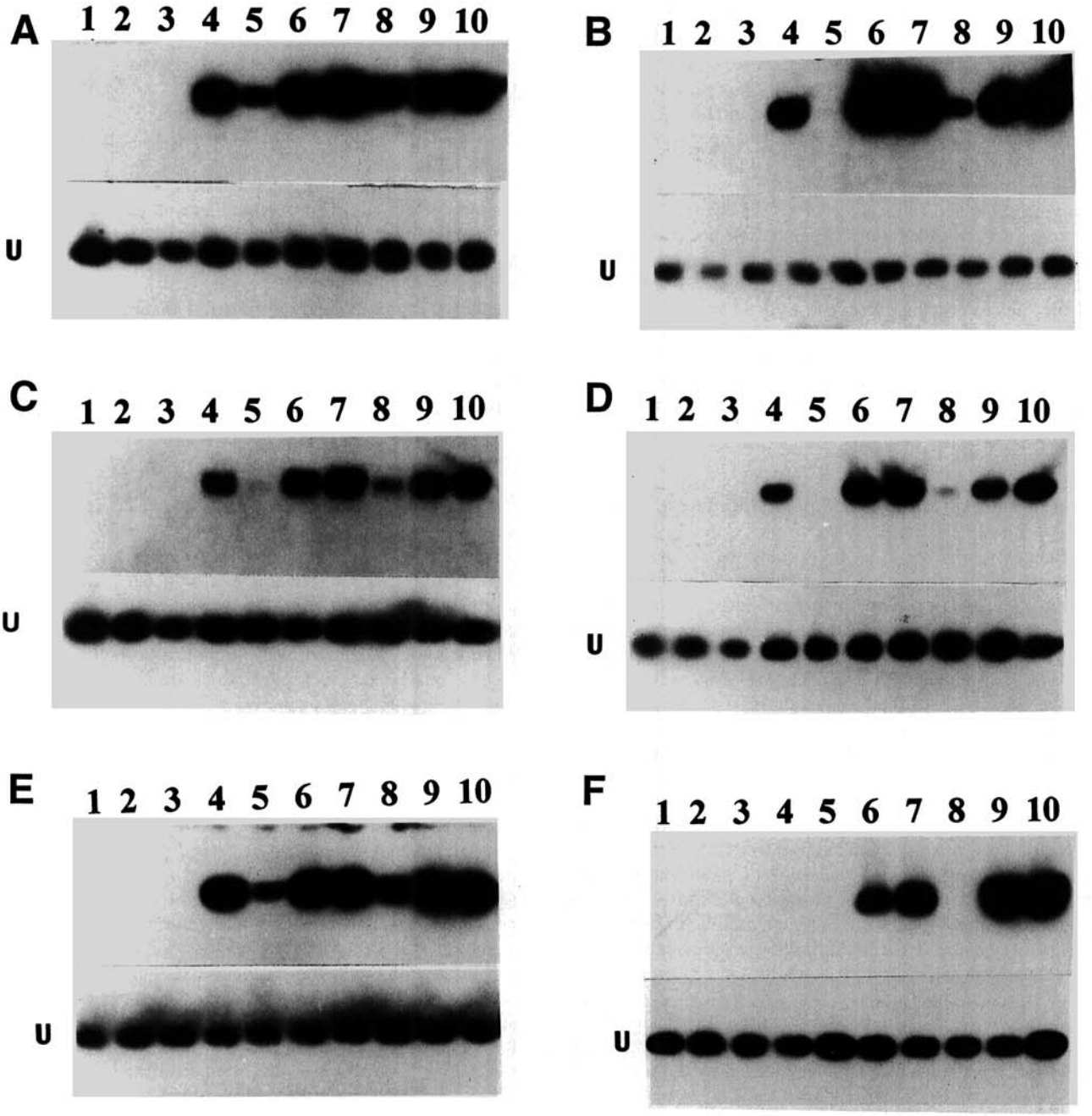

Fig. 4. Expression of nodulin genes in the nodules induced by *ndv* mutants. Total RNAs were isolated from the nodules 8, 14, and 21 days postinoculation (PI) and further processed for reverse transcription–polymerase chain reaction (RT-PCR) with primers specific to ENOD2, ENOD55-1, *Gm*N70, *Gm*N93, NOD26, and Leghemoglobin-a (Lba) with an internal control, ubiquitin (U). The amplified products were separated on agarose gel and probed with each relevant cDNAs. **A,** ENOD2; **B,** nodulin 26; **C,** ENOD55-1; **D,** *Gm*N70; **E,** *Gm*N93 and **F,** Lba. Lane 1, mock inoculated control; lanes 2, 3, and 4, RT-PCR of total RNA from nodules induced by strain AB-1 *(ndvC)* at 8, 14, and 21 days PI, respectively; lanes 5, 6, and 7, RT-PCR of total RNA from nodules induced by strain AB-14 *(ndvB)* at 8, 14, and 21 days PI, respectively; lanes 8, 9, and 10, RT-PCR of total RNA from nodules induced by wild-type strain USDA110 at 8, 14, and 21 days PI, respectively. In each case, the ubiquitin control blot (U) is shown below the nodulin blot.

nodulin expression and nodule development in the *ndvB* mutant AB-14 lags behind that of wild-type–induced nodules until 14 days PI. The primary difference at 14 days PI is that few bacteria are found in the infected cells of nodules induced by strain AB-14. By 21 days PI, the AB-14 induced–nodules have characteristics similar to those of the nodules induced by the wild type. Bacteria were persistent within infected cells and the number of infected cells was increased. However, several characteristics of the AB-14–induced nodules at 21 days PI do differentiate them from the wild type–induced nodules. First, the bacteria were localized to a small area of the cell even though the number of bacteria in this area was high. This localization of bacteria within the plant cell likely coincides with the infection thread. Second, the infected cells remain highly vesiculate. The fact that ENOD2 expression can be detected at 8 days PI is also noteworthy. This nodulin is thought to be a molecular marker for parenchyma cell differentiation resulting in the sclerification of a tissue layer that ultimately serves as the oxygen barrier for the nodule (van de Wiel et al. 1990b). Therefore, this oxygen barrier may exist in nodules induced by strain AB-14, although these nodules are unable to fix nitrogen.

Unlike the AB-14 (*ndvB*) mutant, the AB-1(*ndvC*) mutant retains the ability to produce cyclic β-glucans; however, they are structurally altered and are primarily β-(1→3) linked. The formation of nodulelike structures by strain AB-1 was rare when assays were done at 14 days PI. However, nodulelike structures were evident when the strain was examined at 21 days PI, and all the nodulins tested (except Lba) were expressed. The nodules induced by the AB-1 mutant are also unusual in that they were small, white structures that lacked bacteria and infection threads. At 21 days PI, both early and late nodulins were detected and some tissue differentiation was apparent. At a very rudimentary level, the observed differentiation was similar to that found in wild-type–induced nodules in that the inner and outer parenchyma layers were apparently separated by a layer of sclerified cells. This suggests that the structures induced by the AB-1 mutants represent partially differentiated nodules. However, other factors suggest that development in these structures was halted at some early stage. The early nodulin ENOD2 expressed in these aberrant nodules has been shown in wild-type nodules to be localized to the parenchyma cortical cells and is a marker for differentiation of the sclerified tissue layer (van de Wiel et al. 1990b). As discussed above, the AB-1–induced nodules showed parenchyma cell differentiation. Tissue from the central region of the nodules, however, does not differentiate into infected and uninfected cell types. The lack of Lba expression provides corroborative support for this lack of tissue differentiation. Some morphological features of the nodules formed by the AB-1 mutant are similar to those found in plants exhibiting a defense response to pathogen attack. The more pronounced endodermis and the thickened cell walls in the central region are both characteristics of a plant defense response. These data suggest that the AB-1 mutant may induce nodule development to a point at which the plant mounts a defensive response to infection. Indeed, Mithofer et al. (in press) showed that *B. japonicum* cyclic β-(1→3,1→6)glucan can suppress a fungal β-glucan–induced plant defense response in soybean. It may be that the glucan produced by strain AB-1, lacking β-(1→6) glycosidic linkages, is unable to suppress a plant defense response in soybean or, indeed, may induce a defense response (Miller et al. 1994).

MATERIALS AND METHODS

Plant and bacterial culture.

Glycine max (L.) Merr. 'Essex' seeds were surface sterilized and germinated for 2 days in the dark as described by Nieuwkoop et al. (1987). Seedlings were transferred to plastic growth pouches (Vaughan's Co., Downers Grove, IL) and grown in a chamber with a cycle of 16 h light at 26°C and 8 h dark at 20°C for 2 days. *B. japonicum* strain USDA110 and the two *ndv* mutants (AB-14 [*ndvB]* and AB-1 [*ndvC]*) were grown in HM medium containing (Cole and Elkan 1973) fructose (100 mM) and chloramphenicol (30 μg/ml) with or without streptomycin and kanamycin (100 μg/ml each), respectively. Plant roots were inoculated at 1×10^9 cells per plant. Plants were returned to the growth chamber and examined periodically.

Reverse transcription and polymerase chain reaction.

Total RNAs were isolated from the nodules (at least four plants) by the hot phenol method (Kohrer and Domdey 1991). In the case of roots inoculated with the *ndvC* mutant, strain AB-1, nodulelike structures appearing at 14 and 21 days PI were used for RNA isolation. At 8 days PI, whole roots were used to isolate RNA because no visible structure was induced by this strain. RNA was processed for PCR reaction as described by Minami et al. (in press). In brief, after treatment with RNAse-free DNAse I (Promega Co., Madison, WI), 0.5 μg of total RNA was reverse transcribed by M-MLV reverse transcriptase (United States Biochem. Co., Cleveland, OH) with oligo$(dT)_{12\text{-}18}$ as a primer, according to the manufacturer's manual. Products were recovered by ethanol precipitation after addition of 10 μg of glycogen (Boehringer Mannheim Co., Indianapolis, IN), dissolved in 50 μl of sterile H_2O, and frozen until further analysis. An aliquot (5 μl) was utilized for PCRs in the presence of 10 mM Tris-HCl (pH 8.0), 50 mM KCl, 2.5 mM $MgCl_2$, 1 unit of *Taq* DNA polymerase (Promega) in 30 cycles of PCR (94°C, 1 min, 55°C, 1.5 min, 72°C, 1.5 min) with 10 min of extension time at 72°C. The

Table 1. Polymerase chain reaction primers used in this study

Nodulin	Forward (5′–3′)	Reverse (5′–3′)	Expected size	Reference
ENOD2	CGCTATCCACCATCCAACAA	TAGAGTATTATACATAGGCA	189 bp	Franssen et al. 1989
ENOD55-1	AATGAGACGGATTATGAACA	AAATGCATGCTTGACCT	78 bp	de Blank et al. 1993
*Gm*N93	GTTGCCTCTGCCATTCC	TGCTATCCATTCGGATTCAT	207 bp	Kouchi and Hata 1993
*Gm*N70	CTTTAATGAGCTTCAAGTGA	AATGATACCACTTCTCTATT	237 bp	Kouchi and Hata 1993
NOD26	TTCCTCATGTTCGTCATAT	GAGGAAAGAAGCACTCTT	297 bp	Fortin et al. 1987
Lba	ATTCCTCAATACAGCGT	TGCTTTTTGGGCATGAAC	225 bp	Hyldig-Neilson et al. 1982
Ubiquitin	GGGTTTTAAGCTCGTTGT	GGACACATTGAGTTCAAC	129 bp	Fortin et al. 1988

sequence of the primers used for PCR is listed in Table 1. As an internal control, PCR was also performed simultaneously as described by Horvath et al. (1993) with primers identical in sequence to the soybean ubiquitin gene (Fortin et al. 1988). PCR products were separated by electrophoresis on a 1.5% (wt/vol) agarose gel followed by blotting to a nylon membrane (Hybond-N, Amersham Corp., Arlington Heights, IL). The PCR products were detected by hybridization with ^{32}P-labeled relevant cDNA. In the control experiments, RNA was treated in the same way without reverse transcriptase, and no significant signal after hybridization was detected (data not shown).

Electron microscopic observation.

Soybean nodules 14 or 21 days PI were excised from roots with a razor blade. A portion of the root was retained to help with subsequent orientation. All nodules were taken from the lateral roots on the upper one-third of the plant root mass. Lateral root nodules were used since this was the location where most of the nodules were formed by the *ndv* mutants. Nodules were fixed with the methods described by Roth and Stacey (1989). Sections were cut with a Reichert OMU 3 ultramicrotome. Semi-thin sections (approximately 1 μm thick) were stained with methylene blue, examined, and photographed with a Nikon microphot optical microscope. Thin sections (approximately 150 nm thick) were stained with uranyl acetate and lead citrate, examined, and photographed with a Hitachi H-600 electron microscope operating at 75kV.

ACKNOWLEDGMENTS

We thank Hiroshi Kouchi of the National Institute of Agrobiological Resources of Japan for his kind supply of cDNA clones for soybean nodulins and Naoko Ishii-Minami of the University of Tennessee for her technical support and invaluable encouragement. This work was supported in part by a grant to G.S. from the U.S. Department of Energy (92ER20072) and a grant to D.L.K. and A.A.B. from the USDA NRI Competitive Research Program (#93-37305-9233).

LITERATURE CITED

Bately, M., Redmond, J. W., Djordjevic, S. P., and Rolfe, B. G. 1987. Characterization of glycerophosphorylated cyclic β-(1→2)-glucans from a fast-growing *Rhizobium* species. Biochim. Biophys. Acta 901: 119-126.

Bhagwat, A. A., Gross, K. C., Tully, R. E., and Keister, D. L. β-glucan synthesis in *Bradyrhizobium japonicum*: Characterization of a new locus (*ndvC*) influencing β-(1→6) linkages. J. Bacteriol. (In press.)

Bhagwat, A. A., and Keister, D. L. 1995. Site-directed mutagenesis of the β-(1→3), β-(1→6)-D-glucan synthesis locus of *Bradyrhizobium japonicum*. Mol. Plant-Microbe Interact. 8:366-370.

Bhagwat, A. A., Tully, R. E., and Keister, D. L. 1993. Identification and cloning of cyclic β-(1→3), (1→6)-D-glucan synthesis locus from *Bradyrhizobium japonicum*. FEMS Microbiol. Lett. 114:139-144.

Breedveld, M. W., and Miller, K. J. 1994. Cyclic β-glucans of members of the family Rhizobiaceae. Microbiol. Rev. 58:145-161.

Cole, M. A., and Elkan, G. H. 1973. Transmissable resistance to penicillin G, neomycin, and chloramphenicol in *Rhizobium japonicum*. Antimicrob. Agents Chemother. 4:248-253.

de Blank, C., Mylona, P., Yang, W. C., Katinakis, P., Bisseling, T., and Franssen, H. 1993. Characterization of the soybean early nodulin cDNA clone GmENOD55. Plant Mol. Biol. 22:1167-1171.

Dylan, T., Helinski, D. R., and Ditta, G. S. 1990a. Hypoosmotic adaptation in *Rhizobium meliloti* requires β-(1-2)-glucan. J. Bacteriol. 172: 1400-1408.

Dylan, T., Ielpi, L., Stanfield, S., Kashyap, L., Douglas, C., Yanofsky, M., Nester, E., Helsinki, D. R., and Ditta, G. 1986. *Rhizobium meliloti* genes required for nodule development are related to chromosomal virulence genes in *Agrobacterium tumefaciens*. Proc. Natl. Acad. Sci. USA 83:4403-4407.

Dylan, T., Nagpal, P., Helinski, D. R., and Ditta, G. S. 1990b. Symbiotic pseudorevertants of *Rhizobium meliloti ndv* mutants. J. Bacteriol. 172: 1409-1417.

Finan, T. M., Hirsch, A. M., Leigh, J. A., Johansen, E., Kuldau, G. A., Deegan, S., Walker, G. C., and Signer, E. R. 1985. Symbiotic mutants of *Rhizobium meliloti* that uncouple plant from bacterial differentiation. Cell 40:869-877.

Fortin, M. G., Morrison, N. A., and Verma, D. P. S. 1987. Nodulin 26, a peribacteroid membrane nodulin is expressed independently of the development. Nucleic Acids Res. 15:813-814.

Fortin, M. G., Purohit, S. H., and Verma, D. P. S. 1988. The primary structure of soybean (*Glycine max*) ubiquitin is identical to other plant ubiquitins. Nucleic Acids Res. 16:11377.

Franssen, H. J., Thompson, D. V., Idler, K., Kormelink, R., van Kammen, A., and Bisseling, T. 1989. Nucleotide sequence of two soybean ENOD2 early nodulin genes encoding Ngm-75. Plant Mol. Biol. 14: 103-106.

Hisamatsu, M., Yamada, T., Higashiura, T., and Ikeda, M. 1987. The production of acidic, O-acetylated cyclosophorans (cyclic β-(1→2)-D-glucans) by *Agrobacterium* and *Rhizobium* species. Carbohydr. Res. 163:115-122.

Horvath, B., Heidstra, R., Lados, M., Moerman, M., Spaink, H. P., Prome, J.-C., van Kammen, A., and Bisseling, T. 1993. Induction of pea early nodulin gene expression by nod factors of *Rhizobium*. Plant J. 4:727-733.

Hyldig-Nielsen, J. J., Jensen, E. O., Paludan, K., Wiborg, O., Garrett, R., Jorgensen, P., and Marcker, K. A. 1982. The primary structure of two leghemoglobin genes from soybean. Nucleic Acids Res. 10:689-701.

Ielpi, L., Dylant, T., Ditta, G. S., Helinski, D. R., and Stanfield, S. W. 1990. The *ndvB* locus of *Rhizobium meliloti* encodes a 319-kDa protein involved in the production of β-(1→2)-glucan. J. Biol. Chem. 265:2843-2851.

Kohrer, K., and Domdey, H. 1991. Preparation of high molecular weight RNA. Methods Enzymol. 194:398-405.

Kouchi, H., and Hata, S. 1993. Isolation and characterization of novel nodulin cDNAs representing genes expressed at early stages of soybean nodule development. Mol. Gen. Genet. 238:106-119.

Leigh, J. A., Reed, J. W., Hanks, J. F., Hirsch, A. M., and Walker, G. C. 1987. *Rhizobium meliloti* mutants that fail to succinylate their calcofluor-binding exopolysaccharide are defective in nodule invasion. Cell 51:579-587.

Leigh, J. A., Signer, E. R., and Walker, G. C. 1985. Exopolysaccharide-deficient mutants of *Rhizobium meliloti* that form ineffective nodules. Proc. Natl. Acad. Sci. USA 82:6231-6235.

Miller, K. J., and Gore, R. S. 1992. Cyclic β-(1→6)(1→3)-glucans of *Bradyrhizobium japonicum*: functional analogs of the cyclic β-(1,2)-glucans of *Rhizobium*? Curr. Microbiol. 24:101-104.

Miller, K. J., Hadley, J. A., and Gustine, D. L.. 1994. Cyclic β-(1→6)(1→3)-glucans of *Bradyrhizobium japonicum* USDA110 elicit isoflavonoid production in the soybean host. Plant Physiol. 104:917-923.

Minami, E., Kouchi, H., Cohn, J. R., Ogawa, T., and Stacey, G. Expression of the early nodulin, ENOD40, in soybean roots in response to various lipo-chitin signal molecules. Plant J. (In press.)

Mithofer, A., Bhagwat, A. A., Feger, M., and Ebel, J. Suppression of fungal -glucan-induced plant defense in soybean (*Glycine max* L.) by cyclic β-(1→6)(1→3)-glucans from the symbiont *Bradyrhizobium japonicum*. Planta (In press.)

Nieuwkoop, A., Banfalvi, Z., Deshmane, N., Gerhold, D., Schell, M., Sirotkin, K., and Stacey, G. 1987. A locus encoding host range is linked to the common nodulation genes of *Bradyrhizobium japonicum*. J. Bacteriol. 169:2631-2638.

Rolin, D. B., Pfeffer, P. E., Osman, S. F., Szwergold, B. S., Kappler, F., and Benesi, A. J. 1992. Structural studies of a phosphocholine substituted β-(1→3)(1→6) macrocyclic glucan from *Bradyrhizobium japonicum* USDA110. Biochim. Biophys. Acta 1116:215-225.

Rossbach, S., Gloudemans, T., Bisseling, T., Studer, D., Kaluza, B., Ebeling, S., and Hennecke, H. 1989. Genetic and physiologic characterization of a *Bradyrhizobium japonicum* mutant defective in early bacteroid development. Mol. Plant Microbe Interact. 2:233-240.

Roth, L. E., and Stacey, G. 1989. Bacterium release into host cells of nitrogen-fixing soybean nodules: The symbiosome membrane comes from three sources. Eur. J. Cell Biol. 49:13-23.

Roth, L. E., and Stacey, G. 1992. Rhizobium-legume symbiosis. Pages 255-301 in: Microbial Cell-Cell Interactions. M. Dworkin, ed. American Society of Microbiology, Washington, DC.

Stanfield, S. W., Ielpi, L., O'Brochta, D., Helinski, D. R., and Ditta, G. S. 1988. The *ndvA* gene product of *Rhizobium meliloti* is required for β-(1→2) glucan production and has homology to the ATP-binding export protein HlyB. J. Bacteriol. 170:3523-3530.

van de Wiel, C., Norris, J. H., Bochenek, B., Dickstein, R., Bisseling, T. and Hirsch, A. M. 1990a. Nodulin gene expression and ENOD2 localization in effective, nitrogen-fixing and ineffective, bacteria-free nodules of alfalfa. Plant Cell 2:1009-1017.

van de Wiel, C., Scheres, B., Franssen, H., Van Lierop, M.-J., Van Lammeren, A., Van Kammen, A., and Bisseling, T. 1990b. The early nodulin transcript ENOD2 is located in the nodule parenchyma (inner cortex) of pea and soybean root nodules, EMBO J. 9:1-7.

York, W. S., McNeil, M., Darvill, A.G., and Albersheim, P. 1978. β-2-linked glucans secreted by fast-growing species of *Rhizobium.* J. Bacteriol. 142:243-248.